Detection of Microcalcifications in Mammograms using Multi-chromosome Cartesian Genetic Programming

Julian F. Miller
Dept. of Electronics
University of York
York, YO10 5DD, UK
+44 1904 432383
jfm7@ohm.york.ac.uk

Stephen L. Smith
Dept. of Electronics
University of York
York, YO10 5DD, UK
+44 1904 432351
sls5@ohm.york.ac.uk

Yuan Zhang
Dept. of Electronics
University of York
York, YO10 5DD, UK
+44 1904 432830
yz516@ohm.york.ac.uk

ABSTRACT
Mammograms are high resolution x-rays of the breast that are widely used to screen for cancer in women. This paper describes the first stage of development of a novel representation of Cartesian Genetic Programming as part of a computer aided diagnostic system. Specifically, this work is concerned with automated recognition of microcalcifications, one of the key structures used to identify cancer. Results are presented for the application of the proposed algorithm to a number of mammogram sections taken from the Lawrence Livermore National Laboratory database. These demonstrate the proposed representation is effective in locating microcalcifications and will provide a promising basis on which to conduct future work in discriminating between microcalcifications that are indicative of cancer and those that are not.

Categories and Subject Descriptors
I.2.1 [**Artificial Intelligence**]: Applications and Expert Systems – *Medicine and science.*

General Terms
Algorithms, Experimentation.

Keywords
Mammography, Cartesian Genetic Programming, Genetic Programming.

1. INTRODUCTION
Mammograms are high resolution x-rays of the breast that are routinely used to screen for cancer in women. One important feature used to indicate the presence of cancer are microcalcifications - small deposits of calcium within the breast tissue. This paper describes the development of a novel evolutionary algorithm to locate microcalcifications, in digitized mammograms as the first stage of a diagnostic system.

GECCO'10, July 7–11, 2010, Portland, Oregon, USA.

Breast cancer is one of the leading causes of death in women in the western world. In 2005, some 40,000 new cases were detected in the UK alone and 10,300 women died as a result of the disease [2] making it the most common cancer in women and the second most common cause of death through cancer. The number of breast cancer related deaths has fallen since screening programmes were introduced in 1988. Nonetheless, it is predicted that one in seven women will develop breast cancer at some point during their life [10].

The detection of breast cancer in the early stages of the disease significantly increases the survival rate of patients. The main method for screening patients is the mammogram, a high resolution x-ray of the breast [1]. The process of identifying and evaluating signs of cancer from mammograms is a very difficult and time-consuming task that requires skilled and experienced radiologists. This assessment is also, by its nature, highly subjective and susceptible to error, leading to cancers being missed and the patients misdiagnosed. To achieve a more accurate and reliable diagnosis, Computer Aided Detection (CAD) systems have been investigated which provide an objective, quantitative evaluation. CAD systems have the potential to help in two main ways: (i) the detection of suspicious areas in the mammogram that require further investigation and (ii) the classification of such areas as cancerous (malignant) or non-cancerous (benign) [4].

Two powerful indicators of cancer that are commonly used in evaluating mammograms are known as masses and microcalcifications. Masses are the larger of the two indicators and can be either benign or malignant. Characteristics such as the border and density of the mass, which is greater for malignant examples, can be used for classification. Traditionally, masses are more difficult to classify than microcalcifications. Microcalcifications are essentially small calcium deposits which occur as the result of secretions from ductal structures that have thickened and dried. They can have a great variety of mostly benign causes, but might also be an indication for malignancy. They are fairly common in mammograms and their appearance increases with age, so that they can be found in 8% of mammograms of women in their late 20s and in 86% of mammograms of woman in their late 70s [10]. Microcalcifications that indicate malignancy are usually less than 0.5mm in size and often grouped into clusters of five or more. Any calcification larger than 1mm is almost always benign [10].

The ultimate aim of our work is to assess the potential benefit of a new representation of evolutionary algorithm in the classification of mammograms as part of a CAD system and determine whether further development of such algorithms will lead to a more

confident diagnosis. The aim of this paper, however, is an important step towards this aim, to investigate the suitability of the evolutionary algorithm to reliably detect microcalcifications within the mammogram.

Previous work undertaken in the classification of microcalcifications using evolutionary algorithms is considered in Section 2. The evolutionary algorithm used in the current work will then be described in Section 3 and experiments applying this technique to a number of digitized mammograms will be considered in Section 4. Finally, the potential of the proposed algorithm will be evaluated in Section 5.

2. PREVIOUS WORK

Over recent years there has been much research into the application of CAD to breast cancer with numerous different approaches being exploited and many of these involve image analysis of the digitized mammogram. A typical approach is to use a pattern recognition scheme that employs sensing, segmentation, feature extraction, feature selection and classification, to isolate and then characterize a feature of interest [7]. Each stage of this processing is a potentially complex operation requiring much investigation.

The work described in this paper investigates the use of a novel representation of Cartesian Genetic Programming (CGP), an evolutionary algorithm based on genetic programming [12][13]. Evolutionary algorithms, and in particular, genetic algorithms, have previously been used with success in CAD, but typically only in the feature selection stage of the pattern recognition scheme [5][6][8]. This limited use of evolutionary algorithms prompted the authors to investigate the wider use of CGP in the diagnosis of malignant mammograms and has resulted in a number of promising studies [16][18].

It is the development of this novel representation of CGP, that the authors report in this paper, and specifically, the potential to train the algorithm to successfully locate microcalcifications within the mammogram. It is important to state that the motivation is not merely to detect microcalcifications, but a stage in developing an algorithm that can reliably distinguish between those microcalcifications indicative of cancer (malignant) and those that are not (benign).

To support this and previous investigations by the authors, mammograms have been taken from the Lawrence Livermore National Laboratory database [11]. Regions of interest, featuring at least one microcalcification, have been extracted from the mammogram and stored as a 128 x 128 pixel, 8 bit grayscale image. An example of such a region of interest featuring two microcalcifications is shown in Fig 2.1. To provide a summary of the location of the featured microcalcification(s), each region of interest is divided into 256 equally spaced, non-overlapping, logical parts, as depicted in Fig. 2.2. A respective *parts* file has then been generated for each region of interest, which simply provides the respective number of white (or to be precise, non-zero intensity) pixels for each section of the image. An example parts file is shown in Fig. 2.3, for the region of interest shown in Fig. 2.1.

As will be explained in Section 3, this logical division of the mammogram region of interest into parts is central to the organization and execution of the evolutionary algorithm.

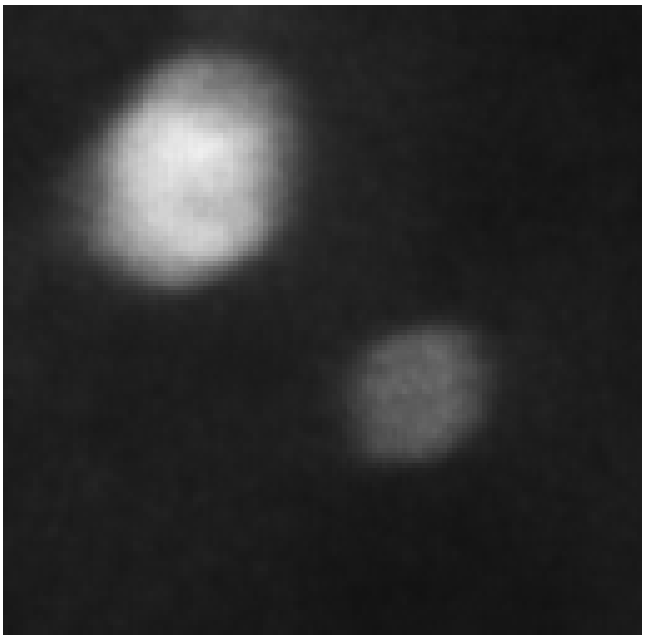

Fig 2.1. Example mammogram region of interest featuring two microcalcifications.

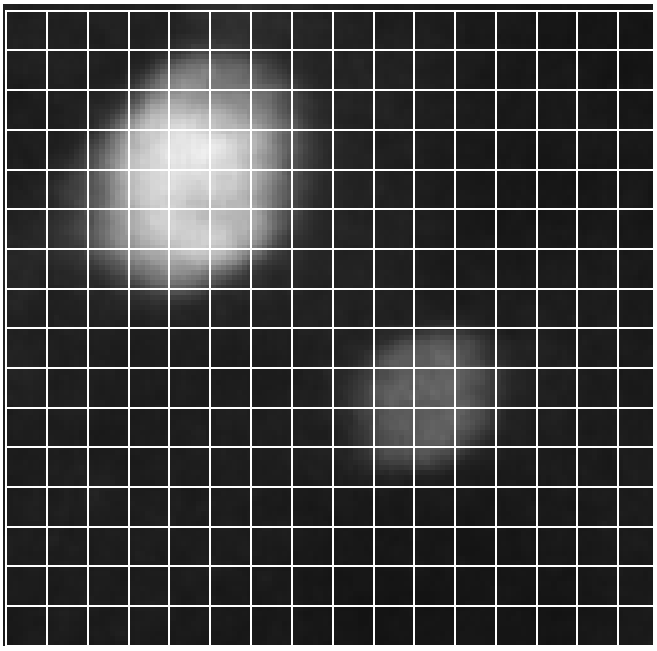

Fig 2.2. Logical division of mammogram region of interest divided into 256, 8x8 pixel parts.

0	0	4	30	13	22	7	0	0	0	0	0	0	0	0	0
0	5	55	64	64	64	60	9	0	0	0	0	0	0	0	0
0	29	64	64	64	64	64	49	0	0	0	0	0	0	0	0
0	44	64	64	64	64	64	64	0	0	0	0	0	0	0	0
0	55	64	64	64	64	64	59	0	0	0	0	0	0	0	0
0	54	64	64	64	64	64	32	0	0	0	0	0	0	0	0
0	30	63	64	64	64	52	4	0	0	0	0	0	0	0	0
0	0	7	32	30	15	0	0	0	0	0	0	0	0	0	0
0	0	0	0	0	0	0	0	0	19	44	53	0	0	0	0
0	0	0	0	0	0	0	0	10	64	64	64	5	0	0	0
0	0	0	0	0	0	0	0	20	64	64	50	0	0	0	0
0	0	0	0	0	0	0	0	3	32	33	7	0	0	0	0
0	0	0	0	0	0	0	0	0	0	0	0	0	0	0	0
0	0	0	0	0	0	0	0	0	0	0	0	0	0	0	0
0	0	0	0	0	0	0	0	0	0	0	0	0	0	0	0
0	0	0	0	0	0	0	0	0	0	0	0	0	0	0	0

Fig 2.3. File representation of white (non-zero intensity) pixel count for respective parts of mammogram region of interest shown in Fig. 2.2.

3. IMPLEMENTATION

CGP is a graph-based genetic programming system which has been shown to perform well within a wide range of problem domains. CGP represents programs using n-dimensional grid (where n is typically 1 or 2) in which each node contains a computational function. Program inputs and outputs are delivered to and taken from specific nodes. Interconnections between functions, inputs and outputs are expressed in terms of the grid's Cartesian co-ordinate system. The 2-D CGP general form is shown in

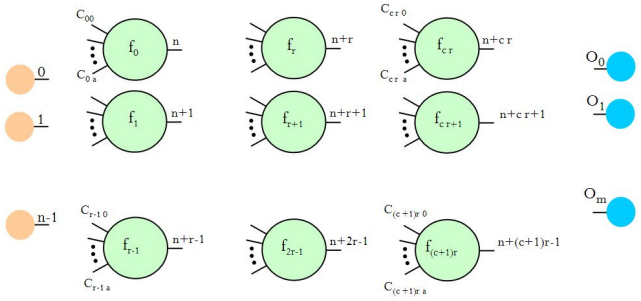

$f_0\ C_{00} \ldots C_{0a} \ \ldots\ f_{(c+1)r}\ C_{(c+1)r\ 0} \ldots C_{(c+1)r\ a} \quad O_1,\ldots O_m$

Fig 3.1. General form of two-dimensional CGP.

All nodes are assumed to take as many inputs as the maximum function arity a (Fig. 1). Every data input and node output are labelled consecutively (starting at 0) which gives it a unique data address which specifies where the input data or node output value can be accessed (shown in the figure on outputs of inputs and nodes). Nodes in columns cannot be connected to each other. The graph is directed so that a node may only have its inputs connected to either input data or the output of a node in a previous column. In general there may be a number of output genes (O_i) which specify where the program outputs are taken from. The structure of the genotype is seen below the schematic. All node functions genes f_i are integer addresses in a user defined look-up table of functions. All connection genes C_{ij} are integers taking values between 0 and the address of the node at the bottom of the previous column of nodes. Nodes can receive program inputs irrespective of position in the grid. There are three important parameters that control the topology of the graphs encoded in CGP. The number of rows (r), the number of columns (c) and a parameter called levels-back (l). This controls how many columns back a node may be connected to. For example if the level-back is one, all nodes in any column can only connect to either a program input or a node in the previous column. A CGP chromosome is a list of integers. Decoding the function of a CGP chromosome consists of following links from the program outputs to the program inputs. Often, when this is carried out, many node outputs are not used. Associated with these nodes are non-coding genes. It is clear that the genotype-phenotype mapping in CGP is highly redundant.

A mutation operator can alter both the function present within a grid cell and the connections between components. In CGP a form of 1+λ evolutionary strategy is often used (as in this paper). This has the form:

1. Generate initial population of 1+λ programs randomly
2. Evaluate fitness of the population
3. Select the fittest of the population as the parent
4. Mutate the parent to generate λ offspring to form the new population
5. Select a new parent using the following rules:
   - 5.1 If any of the offspring have better fitness than the parent, the fittest offspring becomes the new parent
   - 5.2 Else if there are offspring with the same fitness as the parent one of them is randomly selected to be the new parent
   - 5.3 Else, the current parent remains as the parent
6. Go to step 4 unless the maximum number of generations has reached.

CGP chromosomes often have large numbers of non-coding genes [14] and so with sufficiently small numbers of mutations different population members can decode to the same phenotype. This means that step 5.2 happens very often during evolutionary search. Previous studies have verified the great utility of this neutral search [17][19].

In this paper multiple CGP chromosomes are used to evolve a single mammogram. We use a generalized form of the 1+λ evolutionary strategy above in which each *chromosome* is selected using the algorithm above. This has previously been shown to be highly effective [15][16]. The image is divided into equal sized, non-overlapping parts and each one of these is assigned its own CGP chromosome which is evaluated independently.

In this work each genotype consists of 256 independent CGP chromosomes using a grid of 1 rows and 500 columns. Each chromosome has 64 inputs corresponding to an 8x8 grid of grey scale pixel values (0 to 255). Each chromosome has a single

output gene. The mammogram images are divided into 256, 8x8 pixel areas. The 64 grey scale pixel values (0 to 255) for each of these areas form the inputs to an individual CGP network, encoded by a chromosome. The chromosome mutation rate defines the percentage of genes in each chromosome that are mutated when a genotype is mutated. The node functions, f_0 and f_1 are two forms of 2 to 1 multiplexers operating with 8-bit arithmetic. Muliplexers are used because they represent binary IF statements and have been shown previously to be effective when CGP chromosomes operate on binary data [13]. Assuming the 8-bit binary inputs are defined as x, y, and z, the functions are defined as follows:

$$f_0 = x.z' + y.z\ ,\ f_0 = x.z' + y'.z \tag{3.1}$$

where the symbols, . , + and ´, indicate 8-bit bitwise logical AND, OR and complement operations. The experimental parameters used for all evolutionary runs are shown in Table 4. To explain the meaning of mutation rate consider 0.25% mutation. This means that 5 genes were mutated from the parent to make each offspring (0.25% of 500*4+1 genes). Preliminary experiments were conducted that indicated the parameter values we have used worked reasonably well, but were not neccesarily optimal.

The output of the program encoded in each chromosome is automatically an integer between 0 and 256. This is divided by 4. To calculate the fitness of a particular chromosome, i, we apply the 64 grey scale pixel values from a unique section of the image as the input to the encoded program and compare the output of the program, $D_i/4$ with the known number of microcalcifications pixels in the image section (a number between 0 and 64). We denote the latter by M_i. We investigated two fitness function in the work reported in this paper. The linear fitness of a single chromosome, i, on a collection of j = 1 to m, mammograms is defined as follows. This is also the average absolute difference between $D_i/4$ and M_i subtracted from 1 (e.g. if all differences are zero it gets a perfect score of 1).

$$f_i = \frac{1}{m}\sum_{j=1}^{j=m}\left(1 - \left|\frac{D_i}{4} - M_i\right|\right) = 1 - \overline{\left|\frac{D_i}{4} - M_i\right|} \tag{3.2}$$

The nonlinear fitness of a single chromosome we define as follows

$$f_i = \frac{1}{m}\sum_{j=1}^{j=m}\left(\frac{1}{1+|D_i - M_i|}\right) \tag{3.3}$$

We then obtain the fitness of a genotype (consisting of multiple chromosomes) by summing all the chromosome fitnesses and dividing by the number of chromosomes (256). In this way we arrive at a fitness value between 0 and 1 for the entire 256 chromosome genotype. The nonlinear fitness function penalizes differences between the CGP output and the true microcalcification counts to a larger extent than the linear fitness.

4. EXPERIMENTS

Images used in this study are constructed from mammograms in the Lawrence Livermore National Laboratory database that feature microcalcifications [11]. The images have been manually edited and in each case a 128x128 pixel image is constructed containing at least one microcalcification from a particular mammogram. Each image is then logically divided into 256 parts and the status of each part labeled as either being benign or malignant according to the radiologist. In total 31 images were created, of which 13 contained malignant microcalcifications and 18 benign microcalcifications from five separate patients.

The relatively small number of images available to train and test the CGP network has required that k-fold cross validation be used [9]. In k-fold cross validation data is divided into groups called folds and for each training run (i.e. in our case an evolutionary run) all the data in folds except one are used. The data in the fold left out of the training run is used to test the accuracy of the classification program (in our case the results produced by the evolved genotype). This process is then repeated for a new collection of folds. In this way a classification program can be rigourously tested on unbiased unseen test data. For the purpose of this investigation two investigations are considered, each with the data assigned to the folds in a different way. In the first investigation, all images associated with each patient are used to form a separate fold; in the second investigation, images from each patient are distributed across several folds. This assignment is summarized in Tables 1 and 2 and is intended to investigate the power of the algorithm to detect microcalcifications from a particular patient.

Table 1. Patient-centered assignment of images for k-fold cross validation in Experiments 1 and 2. Four folds are used for training and one fold for testing (all combinations tested).

Fold 1	Fold 2	Fold 3	Fold 4	Fold 5
Patient A: Image 1	Patient B: Image 1	Patient C: Image 1	Patient D: Image 1	Patient E: Image 1
Patient A: Image 2	Patient B: Image 2	Patient C: Image 2	Patient D: Image 2	Patient E: Image 2
Patient A: Image 3	Patient B: Image 3	Patient C: Image 3		Patient E: Image 3
	Patient B: Image 4	Patient C: Image 4		
		Patient C: Image 5		
		Patient C: Image 6		

Table 2. Distributed assignment of images for k-fold cross validation in Experiments 3 and 4

Fold 1	Fold 2	Fold 3	Fold 4	Fold 5
Patient D: Image 1	Patient B: Image 1	Patient E: Image 1	Patient D: Image 2	Patient E: Image 2
Patient C: Image 2	Patient E: Image 3	Patient C: Image 6	Patient C: Image 3	Patient C: Image 4
Patient B: Image 2	Patient C: Image 1	Patient B: Image 4	Patient A: Image 3	Patient C: Image 5
Patient A: Image 2	Patient A: Image 1			Patient B: Image 3

For each of these two investigations, both linear and non-linear fitness functions, as described in Section 3, have also been employed, making a total four separate experiments in total, which have been detailed in Table 3. Results for the training of the respective CGP networks are shown in Fig. 4.1 and subsequent testing in Fig.4.2. The parameter values used for the evolution of the CGP networks for each experiment are given in Table 4.

Results for the training of the networks (Fig. 4.1) shows a generally high fitness, but an improved performance using the linear fitness function over the non-linear can be seen. It is apparent, however, that there is little difference in fitness between the patient-centered and distributed k-fold assignment for the cross-validation exercise. This can be interpreted positively, indicating that the CGP networks have evolved a generic microcalcification detector that is not dependent on a particular patient's, or set of patients', examples.

Table 3

Assignment of patient images for k-fold cross validation and use of fitness function in experimental investigations

Experiment	k-folds assignment	Fitness function
1	Patient-centered	Liner
2	Patient-centered	Non-linear
3	Distributed	Liner
4	Distributed	Non-liner

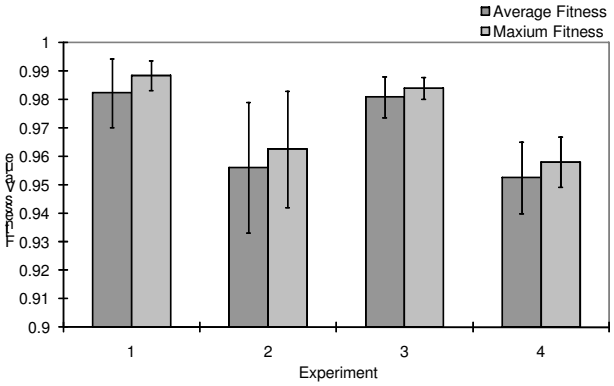

Fig 4.1. Average and maximum fitness values for training of CGP genotypes.

This observation is confirmed when considering the test results for the respective experiments (Fig. 4.2). It is also noted that there is little difference in the test performance between the linear and non-linear trained genotypes, suggesting that the alternative schemes offer little benefit over each other. However, informally we observed toplogical differences between the outputs of the evolved genotypes when looked at in two dimensions. Linear fitness appeared to match contiguous areas of microcalcifications better than nonlinear fitness however it appeared to introduce low level noise in microcalcification counts in areas of the image where no microcalcifications were present. Further analysis of this remains for the future.

It should be noted that although CGP genotypes were trained using non-linear fitness functions in experiments 2 and 4, the linear fitness function was used to evaluate their performance on respective test sets of data to enable fair comparison with those genotypes evolved in experiments 1 and 3.

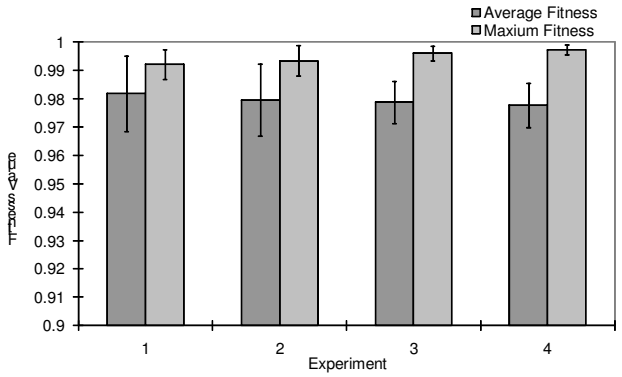

Fig 4.2. Average and maximum fitness values for testing of CGP genotypes.

Table 4

Summary of parameter values used for evolution of CGP genotypes

Parameter	Value
Generations	10000
Population size	5
Mutation rate	0.25
Runs	20
Rows	1
Columns	500
Levels back	500

An example of the microcalcifications detected by the best evolved network is given in Fig. 4.6, which resulted from presenting the test image illustrated in Fig. 4.5 (and Fig. 2.1). The difference in white pixel values obtained between these is summarized in Fig. 4.7 for convenience. These figures give a subjective confirmation that the network has indeed located the microcalcifications within the mammogram region of interest. Although there are differences in the number of white pixels in parts relating to the microcalcifications, there are very few differences in those parts that represent other tissue in the breast, indicating a confident detection.

5. CONCLUSIONS AND FUTURE WORK

This paper has reported the evaluation of a multi-chromosome representation of Cartesian Genetic Programming towards the development of a computer aided diagnostic system for the detection of breast cancer in women. The first stage of this work has been concerned with the detection of microcalcifications, structures commonly used in the diagnosis of cancer in mammograms. Experimental results suggest alternative application of a linear and non-linear fitness function does not affect performance significantly, nor does the distribution of training data in a k-fold cross-validation scheme. The latter suggests that the CGP genotype has evolved effectively, and is able to detect microcalcifications from previously unseen patients.

This is a promising result that encourages further development of the algorithm as part of a computer aided diagnostic system.

In the experiments performed in this paper we evaluate 40,001 genotypes in each evolutionary run. This is a relatively small number. We observed that fitness values continued to improve for longer runs so we would expect even better results on longer runs.

Obtaining exact microcalcification counts is actually less important than indicating contiguous and distinct clusters of microcalcifications. We intend to investigate introducing thresholds for microcalcifications counts in parts, essentially indicating whether they are high or low (above threshold or below). This would mean that fitness would be tested over binary decisions so that the fitness function could utilize true positive, true negative, false positive and false negatives. This would also enable well known techniques such as Receiver Operating characteristics to be used in assessing fitness.

The data sets we have used come from standard, poorish quality and rather old source [11]. We are currently in collaboration with consultants in a local hospital which will shortly install state-of-the-art digital mammography systems. This will no doubt furnish us with much more plentiful high quality data.

Finally, our goal is to diagnose whether patients have malignant or benign microcalcifications, one approach we are considering to allow this is to include an additional chromosome in each part which could be evolved to indicate malignancy or not. These investigations remain for the future.

6. ACKNOWLEDGMENTS

The authors would like to thank Eddy Munday for his work in preprocessing the mammograms used in the experimental work described in this paper.

7. REFERENCES

[1] Andolina, V., Lille, S. and Willison, K. Mammographic Imaging: A Practical Guide. Lippincott-Raven (1993)

[2] Office for National Statistics. http://www.statistics.gov.uk/cci/nugget.asp?id=575

[3] Chan, H., Sahiner, B., Lam, K., Petrick, N., Helvie, M., Goodsitt, M. and Adler, D. Computerized analysis of mammographic microcalcifications in morphological and texture feature space. Medical Physics, vol. 25, no.10, pp. 2007-2019 (1998)

[4] Cheng, H.D., Cai, X., Chen, X. and Hu, L., Lou, X. Computer-aided detection and classification of microcalcifications in mammograms: a survey. Pattern Recognition, vol. 36, pp. 2967 – 2991 (2003)

[5] Fu, J.C. , Lee, S.K., Wong, S.T.C., Yeh, J.Y., Wang, A.H. and Wu, H.K. Image segmentation feature selection and pattern classification for mammographic microcalcifications. Computerized Medical Imaging and Graphics, vol. 29, pp. 419-429 (2005)

[6] Gavrielides, M. Lo, J., Vargas-Voracek, R. and Floyd, C. Segmentation of suspicious clustered microcalcifications in mammograms. Medical Physics, vol 27, pp 13-22 (2000)

[7] Gonzalez, R. and Woods, R. Digital Image Processing, Prentice Hall (2002)

[8] Kim, J. and Park, H. Statistical Textural Features for Detection of Microcalcifications in Digitized Mammograms. IEEE Transactions Medical Imaging, vol. 18, no.3, pp 231-238 (1999)

[9] Kohavi, Ron. A study of cross-validation and bootstrap for accuracy estimation and model selection. Proceedings of the Fourteenth International Joint Conference on Artificial Intelligence. Morgan Kaufmann Vol. 2, No. 12, pp 1137–1143 (1995)

[10] Kopans, D.B., Breast Imaging, Lippincott Williams & Wilkins (2006)

[11] Lawrence Livermore National Laboratory database. https://www.llnl.gov/

[12] Miller, J. F. and Thomson, P.: Cartesian Genetic Programming, Lecture Notes in Computer Science, Vol. 1802, pp.121-132 (2000)

[13] Miller J.F., Job D., Vassilev V.K. Principles in the Evolutionary Design of Digital Circuits - Part I. *Genetic Programming and Evolvable Machines*, Vol. 1, No. 1, pp. 8-35 (2000)

[14] Miller J.F., Smith S.L. Redundancy and Computational Efficiency in Cartesian Genetic Programming. IEEE Transactions on Evolutionary Computation, Vol. 10, pp. 167-174 (2006)

[15] Walker J. A., Miller J. F., Cavill R. A Multi-chromosome Approach to Standard and Embedded Cartesian Genetic Programming, Proceedings of the Genetic and Evolutionary Computation Conference (GECCO), ACM Press, pp. 903-910 (2006)

[16] Walker J. A., Völk K., Smith S. L., Miller J. F. Parallel Evolution using Multi-chromosome Cartesian Genetic Programming, Genetic Programminmg and Evolvable Machines, Vol. 10, No. 4, pp. 417-445, (2010)

[17] Vassilev V. K., Miller J. F. The Advantages of Landscape Neutrality in Digital Circuit Evolution. Proceedings of the 3rd International Conference on Evolvable Systems: From Biology to Hardware. Springer LNCS Vol. 1801, pp. 252-263 (2000)

[18] Völk, K., Miller J. F., Smith, S. L. Multiple Networks CGP for the Classification of Mammograms. Proceedings of the 11th European Workshop on Image Analysis and Signal Processing (EvoIASP'09). Springer LNCS 5484 pp.405-413 (2009)

[19] Yu T., Miller J. F. Neutrality and Evolvability of a Boolean Function Landscape, Proceedings of the 4th European Conference on Genetic Programming (EuroGP2001). Springer LNCS, 2038, pp. 204-217 (2001)

0	0	4	30	13	22	7	0	0	0	0	0	0	0	0	0
0	5	55	64	64	64	60	9	0	0	0	0	0	0	0	0
0	29	64	64	64	64	64	49	0	0	0	0	0	0	0	0
0	44	64	64	64	64	64	64	0	0	0	0	0	0	0	0
0	55	64	64	64	64	64	59	0	0	0	0	0	0	0	0
0	54	64	64	64	64	64	32	0	0	0	0	0	0	0	0
0	30	63	64	64	64	52	4	0	0	0	0	0	0	0	0
0	0	7	32	30	15	0	0	0	0	0	0	0	0	0	0
0	0	0	0	0	0	0	0	0	19	44	53	0	0	0	0
0	0	0	0	0	0	0	0	10	64	64	64	5	0	0	0
0	0	0	0	0	0	0	0	20	64	64	50	0	0	0	0
0	0	0	0	0	0	0	0	3	32	33	7	0	0	0	0
0	0	0	0	0	0	0	0	0	0	0	0	0	0	0	0
0	0	0	0	0	0	0	0	0	0	0	0	0	0	0	0
0	0	0	0	0	0	0	0	0	0	0	0	0	0	0	0
0	0	0	0	0	0	0	0	0	0	0	0	0	0	0	0

Fig 4.5. White pixel count indicating presence of microcalcifications in the original image.

0	0	7	15	7	7	7	0	0	0	0	0	0	0	0	0
0	7	15	31	63	63	31	7	0	0	0	0	0	0	0	0
0	15	31	63	31	63	63	31	0	0	0	0	0	0	0	0
0	15	63	31	15	31	63	31	0	0	0	0	0	0	0	0
0	31	63	31	31	31	63	31	0	0	0	0	0	0	0	0
0	31	63	31	31	31	63	31	0	0	0	0	0	0	0	0
0	7	63	63	63	63	52	4	0	0	0	0	0	0	0	0
0	0	7	31	30	15	0	0	0	0	0	0	0	0	0	0
0	0	0	0	0	0	0	0	0	19	31	31	0	0	0	0
0	0	0	0	0	0	0	0	10	31	15	31	5	0	0	0
0	0	0	0	0	0	0	0	20	31	15	31	0	0	0	0
0	0	0	0	0	0	0	0	3	31	30	7	0	0	0	0
0	0	0	0	0	0	0	0	0	0	0	0	0	0	0	0
0	0	0	0	0	0	0	0	0	0	0	0	0	0	0	0
0	0	0	0	0	0	0	0	0	0	0	0	0	0	0	0
0	0	0	0	0	0	0	0	0	0	0	0	0	0	0	0

Fig 4.6. Microcalcifications detected by the best evolved network.

0	0	-3	15	6	15	0	0	0	0	0	0	0	0	0	0
0	-2	40	33	1	1	29	2	0	0	0	0	0	0	0	0
0	14	33	1	33	1	1	18	0	0	0	0	0	0	0	0
0	29	1	33	49	33	1	33	0	0	0	0	0	0	0	0
0	24	1	33	33	33	1	28	0	0	0	0	0	0	0	0
0	23	1	33	33	33	1	1	0	0	0	0	0	0	0	0
0	23	0	1	1	1	0	0	0	0	0	0	0	0	0	0
0	0	0	1	0	0	0	0	0	0	0	0	0	0	0	0
0	0	0	0	0	0	0	0	0	0	13	22	0	0	0	0
0	0	0	0	0	0	0	0	0	33	49	33	0	0	0	0
0	0	0	0	0	0	0	0	0	33	49	19	0	0	0	0
0	0	0	0	0	0	0	0	0	1	3	0	0	0	0	0
0	0	0	0	0	0	0	0	0	0	0	0	0	0	0	0
0	0	0	0	0	0	0	0	0	0	0	0	0	0	0	0
0	0	0	0	0	0	0	0	0	0	0	0	0	0	0	0
0	0	0	0	0	0	0	0	0	0	0	0	0	0	0	0

Fig 4.7. Difference in number of white pixels signifying microcalcifications in the original image and those detected by the best evolved network.